Denitrification Kinetics of Nitrate by a Heterotrophic Culture in Batch and Fixed-Biofilm Reactors

Authors:

Yen-Hui Lin, Yi-Jie Gu

Date Submitted: 2020-07-07

Keywords: fixed-biofilm, model, batch tests, heterotrophic culture, nitrate reduction, kinetics, denitrification

Abstract:

Herein, the progress of nitrate removal by a heterotrophic culture in a batch reactor and continuous-flow fixed-biofilm reactor was examined. Two batch experiments for nitrate reduction with acetate degradation using 250 mL batch reactors with acclimated denitrifying biomass were conducted. The experimental results indicated that the nitrate was completely reduced; however, the acetate remained at a concentration of 280 mg/L from initial nitrate concentration of 100 mg/L. However, the acetate was fully biodegraded by the denitrifying biomass at an initial nitrate concentration of 300 mg/L. To evaluate the biokinetic parameters, the concentration data of nitrate, nitrite, acetate, and denitrifying biomass from the batch kinetic experiments were compared with those of the batch kinetic model system. A continuous-flow fixed-biofilm reactor was used to verify the kinetic biofilm model. The removal efficiency of nitrate in the fixed-biofilm reactor at the steady state was 98.4% accompanied with 90.5% acetate consumption. The experimental results agreed satisfactorily with the model predictions. The modeling and experimental approaches used in this study could be applied in the design of a pilot-scale, or full-scale, fixed-biofilm reactor for nitrate removal in water and wastewater treatment plants.

Record Type: Published Article

Submitted To: LAPSE (Living Archive for Process Systems Engineering)

Citation (overall record, always the latest version):	LAPSE:2020.0815
Citation (this specific file, latest version):	LAPSE:2020.0815-1
Citation (this specific file, this version):	LAPSE:2020.0815-1v1

DOI of Published Version: https://doi.org/10.3390/pr8050547

processes

MDPI

Article

Denitrification Kinetics of Nitrate by a Heterotrophic Culture in Batch and Fixed-Biofilm Reactors

Yen-Hui Lin * and Yi-Jie Gu

Department of Safety, Health and Environmental Engineering, Central Taiwan University of Science and Technology, 666, Bu-zih Road, Bei-tun District, Taichung 406053, Taiwan

* Correspondence: yhlin1@ctust.edu.tw; Tel.: +886-4-22391647 (ext. 6861)

Received: 28 March 2020; Accepted: 5 May 2020; Published: 8 May 2020

Abstract: Herein, the progress of nitrate removal by a heterotrophic culture in a batch reactor and continuous-flow fixed-biofilm reactor was examined. Two batch experiments for nitrate reduction with acetate degradation using 250 mL batch reactors with acclimated denitrifying biomass were conducted. The experimental results indicated that the nitrate was completely reduced; however, the acetate remained at a concentration of 280 mg/L from initial nitrate concentration of 100 mg/L. However, the acetate was fully biodegraded by the denitrifying biomass at an initial nitrate concentration of 300 mg/L. To evaluate the biokinetic parameters, the concentration data of nitrate, nitrite, acetate, and denitrifying biomass from the batch kinetic experiments were compared with those of the batch kinetic model system. A continuous-flow fixed-biofilm reactor was used to verify the kinetic biofilm model. The removal efficiency of nitrate in the fixed-biofilm reactor at the steady state was 98.4% accompanied with 90.5% acetate consumption. The experimental results agreed satisfactorily with the model predictions. The modeling and experimental approaches used in this study could be applied in the design of a pilot-scale, or full-scale, fixed-biofilm reactor for nitrate removal in water and wastewater treatment plants.

Keywords: denitrification; kinetics; nitrate reduction; heterotrophic culture; batch tests; fixed-biofilm; model

1. Introduction

Nitrate-containing wastewater is often generated from manufacturing processes involving the production of fertilizers, explosives, pectin, cellophane and metals [1,2], which contains nitrate concentrations higher than 1000 mg NO_3−N/L [3]. In addition to industrial activity, the nitrate contamination of ground and surface waters is also associated with recirculating aquaculture systems (RAS). The nitrate concentration in RAS in the range of 100–500 mg/L was reported [4,5]. A wide range of nitrate concentrations from 40 to 1000 mg/L in groundwater was also found in the state of Rajasthan in India [6]. Studies have shown that nitrate concentration exceeds 10 mg/L in many specific wells in Taiwan [7]. Ground and surface waters can be used as the water resource for the purposes of drinking, irrigation, and aquaculture. Thus, the removal of nitrate from ground and surface waters becomes a major concern because of human health risks related to methemoglobinemia; and the possibility of carcinogens in the stomach and intestines [8]. The World Health Organization (WHO) has set a nitrate concentration standard for drinking water of 11.3 mg NO_3–N/L in order to protect water resources and reduce hazards to human health.

Nitrate removal can be achieved by physicochemical processes, e.g., air stripping, breakpoint chlorination, reverse osmosis, and ion exchange. These processes are simple in operation but may cause secondary pollution [2,9]. Heterotrophic denitrifying bacteria utilize various organics such as

methanol, ethanol, acetate, and lactate as the carbon source for biological denitrification, whereas autotrophic denitrifying bacteria use sulfide, sulfur, or hydrogen as the electron donor [10,11].

Biological denitrification, which reduces nitrate (NO_3^-) to nitrogen (N_2) via nitric oxide (NO) and nitrous oxide (N_2O), has been proven to be an effective process for removing nitrogen from its oxidized form [12,13]. The biological denitrification process can be described by the following Equations [12,14]:

$$NO_3^- \rightarrow NO_2^- \rightarrow NO \rightarrow N_2O \rightarrow N_2 \quad (1)$$

Denitrification is carried out by anoxic microorganisms that can use nitrate as a terminal electron acceptor and organic compounds as electron donors for microbial respiration [14,15]. Several commercially available organic compounds have been used as electron donors for denitrification. The commonly used carbon source (electron donor) includes methanol, ethanol, acetic acid, acetate, and methane [12].

The aim of this work was to conduct the continuous-flow fixed-biofilm reactor to treat synthetic nitrate-containing wastewater to meet the requirement of discharge standard of 11.3 mg NO_3-N/L in Taiwan. Moreover, in this study, the synthetic wastewater with an initial concentration of 100–300 mg NO_3-N/L was prepared to simulate the nitrate concentration in recirculating aquaculture systems (RAS) and groundwater. The batch and continuous-flow column tests were conducted to determine the biokinetic parameters for the validation of the kinetic biofilm model. The objectives of this study were to (1) evaluate nitrate elimination by denitrifying biomass using synthetically produced wastewater under various nitrate concentrations in batch tests; (2) determine the biokinetic parameters (μ_{m,NO_3}, Y_{NO_3}, Y_{Ace-NO_3}, K_{S,NO_3}, and b_{NO_3}) for nitrate reduction with acetate degradation by batch tests; (3) determine the biokinetic parameters (μ_{m,NO_2}, Y_{NO_2}, Y_{Ace-NO_2} K_{S,NO_2}, and b_{NO_2}) by fitting experimental results with a batch kinetic model system; (4) develop a mathematical model capable of describing nitrate reduction with acetate degradation from continuous-flow fixed-biofilm column tests; and (5) compare the experimental data and model predictions of effluent concentrations of nitrate, nitrite, acetate, and suspended denitrifying biomass in the fixed-biofilm reactor. The insight on denitrification kinetics gained in this study can be helpful for understanding the behavior of nitrate reduction with acetate degradation with respect to the biological process and the time-variation in component concentrations in the system.

2. Kinetic Model

2.1. Batch Kinetic Model

Biological denitrification is accomplished through consecutive reduction by mixed heterotrophic cultures. The denitrifying bacteria react differently when exposed to different initial nitrate concentrations and other conditions. Thus, many studies were conducted to investigate the behavior of denitrifying bacteria in different concentrations and under various environmental conditions so that the model and experimental results would be useful in the design and optimization of the denitrification process. Knowledge of both kinetics and model development is essential for understanding the process performance. The kinetics of heterotrophic denitrification has been investigated extensively in recent years owing to its beneficial application in bioreactor design and process operation. In this work, it was assumed that microbial growth followed the Monod kinetics, with nitrate and nitrite being the limiting substrates. This is a valid assumption because acetate was provided in excess in all experiments. The Monod growth kinetic expressions applied for nitrate, nitrite, and acetate utilization as well as biomass growth are represented as follows [16]:

$$\frac{dS_{NO_3}}{dt} = -\frac{1}{Y_{NO_3}}\left(\frac{\mu_{m,NO_3} S_{NO_3}}{K_{s,NO_3} + S_{NO_3}}\right)X \quad (2)$$

$$\frac{dS_{NO_2}}{dt} = \frac{1}{Y_{NO_3}}\left(\frac{\mu_{m,NO_3} S_{NO_3}}{K_{S,NO_3} + S_{NO_3}}\right)X - \frac{1}{Y_{NO_2}}\left(\frac{\mu_{m,NO_2} S_{NO_2}}{K_{S,NO_2} + S_{NO_2}}\right)X \quad (3)$$

$$\frac{dS_{Ace}}{dt} = -\frac{1}{Y_{Ace-NO_3}}\left(\frac{\mu_{m,NO_3}S_{NO_3}}{K_{S,NO_3}+S_{NO_3}}\right)X - \frac{1}{Y_{Ace-NO_2}}\left(\frac{\mu_{m,NO_2}S_{NO_2}}{K_{S,NO_2}+S_{NO_2}}\right)X \quad (4)$$

$$\frac{dX}{dt} = \left(\frac{\mu_{m,NO_3}S_{NO_3}}{K_{S,NO_3}+S_{NO_3}} - b_{NO_3}\right)X + \left(\frac{\mu_{m,NO_2}S_{NO_2}}{K_{S,NO_2}+S_{NO_2}} - b_{NO_2}\right)X \quad (5)$$

where S_{NO_3}, S_{NO_2} and S_{Ace} are the concentrations (mg/L) of nitrate, nitrite, and acetate, respectively, in the batch reactor; μ_{m,NO_3} and μ_{m,NO_2} are the maximum specific growth rates (1/d) of biomass on nitrate and nitrite, respectively, in the batch reactor; K_{S,NO_3} and K_{S,NO_2} are the Monod half-saturation constants (mg/L) for nitrate and nitrite, respectively; Y_{NO_3} and Y_{NO_2}, are the biomass yields (mg biomass/mg substrate) of nitrate and nitrite, respectively; Y_{Ace-NO_3} and Y_{Ace-NO_2} are the acetate biomass yields (mg cell/mg substrate) on nitrate and nitrite reductions, respectively; b_{NO_3} and b_{NO_2} are the decay coefficients (1/d) for nitrate and nitrite reductions, respectively; and X is the biomass concentration (mg biomass/L).

Biological denitrification was assumed as a two-step process of nitrate reduction to nitrite, followed by nitrite reduction to nitrogen gas without accumulation of intermediate gaseous products [9]. In the batch tests, the measurements of concentration profiles verified this assumption. This assumption was also used by other researchers to simplify the kinetic model system. The microbial growth in the batch tests was assumed to be subject to a double-substrate limitation by the nitrate and nitrite in steps one and two [16]. The growth of denitrifying bacteria was not inhibited by nitrate [9].

2.2. Determination of Biokinetic Parameters

Equations (2)–(5) were solved simultaneously by using Gear's method [17]. The Gear's method coded in Fortran subroutine was used to integrate the resulting system of first-order ordinary differential equations. The values of various biokinetic parameters (μ_{m,NO_2}, Y_{NO_2}, Y_{Ace-NO_2} K_{S,NO_2}, and b_{NO_2}) were determined by fitting the experimental data with initial concentrations of 100 and 300 mg NO_3-N/L and 590 mg acetate/L at 28° ± 0.2 °C into the batch kinetic model. The average least square provides a quantitative comparison of the agreement between model predictions and experimental data. A large average least square value (LSV) represents less agreement between predicted and experimental data. The LSV is expressed by the following equation [16]:

$$LSV = \frac{1}{N}\sum_{i=1}^{N}\left[\begin{array}{l}\sqrt{\frac{\left(S_{i-NO_3-predicted}-S_{i-NO_3-measured}\right)^2}{\left(S_{i-NO_3-measured}\right)^2}} + \sqrt{\frac{\left(S_{i-NO_2-predicted}-S_{i-NO_2-measured}\right)^2}{\left(S_{i-NO_2-measured}\right)^2}} \\ + \sqrt{\frac{\left(S_{i-Ace-predicted}-S_{i-Ace-measured}\right)^2}{\left(S_{i-Ace-measured}\right)^2}} + \sqrt{\frac{\left(S_{i-X-predicted}-S_{i-X-measured}\right)^2}{\left(S_{i-X-measured}\right)^2}}\end{array}\right] \quad (6)$$

2.3. Biofilm Kinetic Model

Several assumptions of the kinetic biofilm model include the following: (1) the glass beads are spherical; (2) the biofilm is homogeneous and its density is constant; (3) a completely-mixed condition occurred in the bulk liquid; (4) there is no adsorption on glass beads; (5) no inhibition on the growth of denitrifying biomass occurred due to nitrate concentration; (6) diffusion of nitrate, nitrite, and acetate in the biofilm is based on Fick's second law; and (7) acetate is the electron donor and nitrate is the electron acceptor for the growth of the denitrifying biomass [11]. Figure 1 shows the conceptual model for a biofilm attachment on a glass bead.

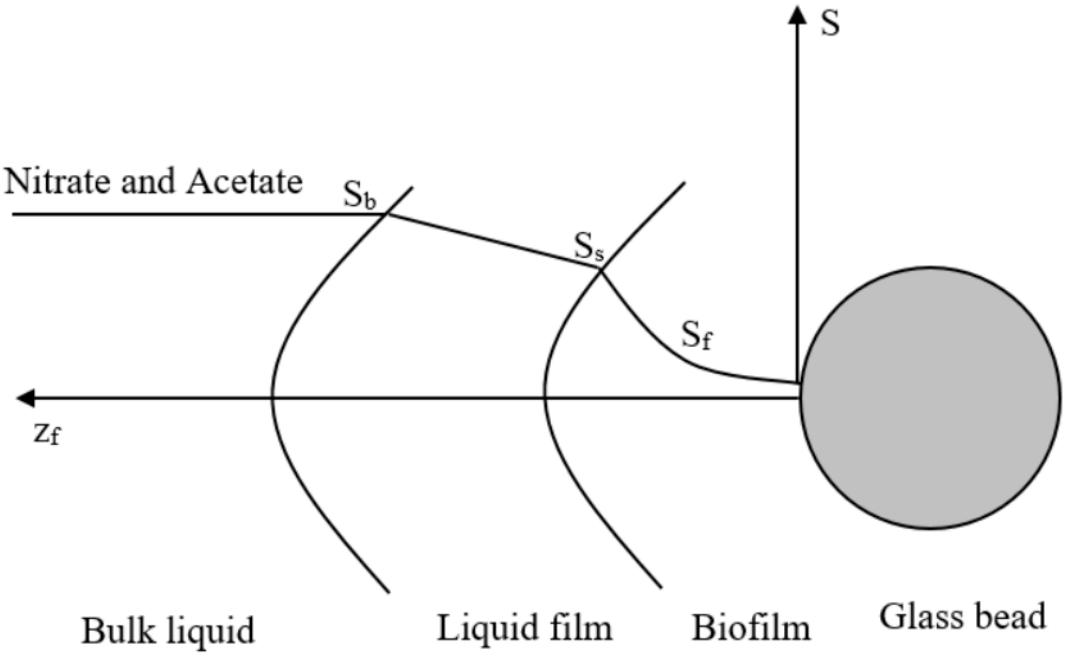

Figure 1. Conceptual model for nitrate and acetate concentration profiles along coordinate system.

A reliable design model used to predict denitrification must be able to provide evaluations of the effluent concentrations of nitrate, nitrite, and acetate and the growths of denitrifying biomass. The simultaneous diffusion and biodegradation for nitrate, nitrate, and acetate in the biofilm are described by the following equation [18]

Nitrate reduction:

$$\frac{\partial S_{f,NO_3}}{\partial t} = D_{f,NO_3}\frac{\partial^2 S_{f,NO_3}}{\partial z_f^2} - \frac{\mu_{m,NO_3} S_{f,NO_3}}{Y_{NO_3}\left(K_{S,NO_3} + S_{f,NO_3}\right)} X_f \tag{7}$$

Nitrite production:

$$\frac{\partial S_{f,NO_2}}{\partial t} = D_{f,NO_2}\frac{\partial^2 S_{f,NO_2}}{\partial z_f^2} + \frac{\mu_{m,NO_3} S_{f,NO_3}}{Y_{NO_3}\left(K_{S,NO_3} + S_{f,NO_3}\right)} X_f - \frac{\mu_{m,NO_2} S_{f,NO_2}}{Y_{NO_2}\left(K_{S,NO_2} + S_{f,NO_2}\right)} X_f \tag{8}$$

Acetate utilization:

$$\frac{\partial S_{f,Ace}}{\partial t} = D_{f,Ace}\frac{\partial^2 S_{f,Ace}}{\partial z_f^2} - \frac{\mu_{m,NO_3} S_{f,NO_3}}{Y_{Ace-NO_3}\left(K_{S,NO_3} + S_{f,NO_3}\right)} X_f - \frac{\mu_{m,NO_2} S_{f,NO_2}}{Y_{Ace-NO_2}\left(K_{S,NO_2} + S_{f,NO_2}\right)} X_f \tag{9}$$

where S_{f,NO_3}, S_{f,NO_2} and $S_{f,Ace}$ are the concentrations (mg/L) of nitrate, nitrite, and acetate, respectively, in the biofilm; D_{f,NO_3}, D_{f,NO_2} and $D_{f,Ace}$ are the diffusion coefficients (cm^2/d) of nitrate, nitrite, and acetate in the biofilm, respectively; X_f is the density of denitrifying biofilm (mg biomass/mL); and z_f is the radial distance (μm) in the biofilm.

Because the nitrate and nitrite with acetate in the bulk liquid migrate to the interface of liquid film/biofilm and diffuse into the denitrifying biofilm during biodegradation, the denitrifying biofilm utilizes nitrate and nitrite with acetate for biosynthesis and respiration. The net growth rate of denitrifying biofilm is balanced by the decay rate and shear loss rate due to the increase or decrease in denitrifying biomass with time. Since the nitrate and nitrite are the two limiting substrates for the growth of the denitrifying biofilm, the growth rate of the denitrifying biofilm can be expressed as

$$\frac{dL_f}{dt} = \int_0^{L_f} \left(\frac{\mu_{m,NO_3} S_{f,NO_3}}{K_{S,NO_3} + S_{f,NO_3}} + \frac{\mu_{m,NO_2}}{K_{S,NO_2} + S_{f,NO_2}} - b_{NO_3} - b_{NO_2} - b_S \right) dz_f \quad (10)$$

where b_s is the biofilm shear loss coefficient (1/d). A fixed-biofilm process in which the kinetic biofilm model can be employed is a completely-mixed biofilm process. All of the suspended denitrifying biomass at bulk liquid phase is exposed to the same substrate concentration. The mass balances for the nitrate, nitrite, acetate and suspended denitrifying biomass in the bioreactor can be represented by the following equations, respectively:

$$\frac{dS_{b,NO_3}}{dt} = \frac{Q}{V\varepsilon}\left(S_{b0,NO_3} - S_{b,NO_3}\right) - k_{f,NO_3}\left(S_{b,NO_3} - S_{s,NO_3}\right)\frac{A}{V\varepsilon} - \frac{\mu_{m,NO_3} S_{b,NO_3}}{Y_{NO_3}\left(K_{s,NO_3} + S_{b,NO_3}\right)} X_b \quad (11)$$

$$\frac{dS_{b,NO_2}}{dt} = \frac{Q}{V\varepsilon}\left(S_{b0,NO_2} - S_{b,NO_2}\right) - k_{f,NO_2}\left(S_{b,NO_2} - S_{S,NO_2}\right) + \frac{\mu_{m,NO_3} S_{b,NO_3}}{Y_{NO_3}\left(K_{S,NO_3} + S_{NO_3}\right)} X_b - \frac{\mu_{m,NO_2} S_{b,NO_2}}{Y_{NO_2}\left(K_{S,NO_2} + S_{b,NO_2}\right)} X_b \quad (12)$$

$$\frac{dS_{b,Ace}}{dt} = \frac{Q}{V\varepsilon}\left(S_{b0,Ace} - S_{b,Ace}\right) - k_{f,Ace}\left(S_{b,Ace} - S_{s,Ace}\right)\frac{A}{V\varepsilon} - \frac{\mu_{m,NO_3} S_{b,NO_3}}{Y_{Ace-NO_3}\left(K_{S,NO_3} + S_{b,NO_3}\right)} X_b - \frac{\mu_{m,NO_2} S_{b,NO_2}}{Y_{Ace-NO_2}\left(K_{S,NO_2} + S_{b,NO_2}\right)} X_b \quad (13)$$

$$\frac{dX_b}{dt} = \frac{Q}{V\varepsilon}(-X_b) + \left(\frac{\mu_{m,NO_3} S_{b,NO_3}}{K_{S,NO_3} + S_{b,NO_3}} - b_{NO_3} \right) X_b + \left(\frac{\mu_{m,NO_2} S_{b,NO_2}}{K_{s,NO_2} + S_{b,NO_2}} - b_{NO_2} \right) X_b + \frac{A}{V\varepsilon} b_s L_f X_f \quad (14)$$

where S_{b0,NO_3}, S_{b0,NO_2} and $S_{b0,Ace}$ are the concentrations (mg/L) of nitrate, nitrite, and acetate, respectively, in the feed; S_{b,NO_3}, S_{b,NO_2} and $S_{b,Ace}$ are the concentrations (mg/L) of nitrate, nitrite, and acetate, respectively, in the bulk liquid; X_b is the denitrifying biomass concentration (mg/L) in the bulk liquid; Q is the influent flow rate (cm^3/d); V is the effective working volume of reactor (cm^3) and ε is the reactor porosity (dimensionless).

2.4. Model Numerical Solution

Equations (7)–(14) consist of a fixed-biofilm model system for nitrate reduction with acetate degradation in a completely-mixed and continuous-flow bioreactor. The orthogonal collocation method combined with Gear's method was used to solve the equations. The continuous-flow fixed-biofilm equations were used first to normalize by defining various dimensionless variables. A set of normalized equations were obtained from dimensionless variables. Legendre polynomial as a symmetrical polynomial in coordinate was applied to approximate the exact concentration profiles of nitrate and acetate within the biofilm. The collocation points are the roots of the corresponding orthogonal polynomial. They are not equally distributed in the domain of interest. The number of collocation points in the glass bead was fixed as 6. The nonlinear parabolic differential equations (Equations (7)–(9)) were converted to 18 ordinary differential equations. The entire model system including 23 ordinary differential equations was integrated using Gear's method to solve the nitrate and acetate concentration profiles; growth of suspended and attached biomass; effluent concentrations of nitrate, nitrite, and acetate in the bulk liquid; as well as the fluxes diffused into and out of the biofilm.

3. Materials and Methods

3.1. Inoculum and Culture Medium

The heterotrophic denitrifying biomass used in the batch and continuous-flow column tests was obtained from the anoxic compartment of a wastewater treatment plant at Chi-Mei Optoelectronics Corp. in Tainan City of Taiwan. Enrichment cultures were incubated under anoxic conditions. The composition of the medium proposed by Tang et al. [11] was applied in this study. The medium

contains the following ingredients: KNO_3 (1.9 g/L), $NaCH_3COO{\cdot}3H_2O$ (1.0 g/L), NaCl (7.0 g/L), $MgSO_4{\cdot}7H_2O$ (0.68 g/L), $CaCl_2{\cdot}2H_2O$ (0.24 g/L), NH_4Cl (0.02 g/L); KH_2PO_4 (0.027 g/L); $NaHCO_3$ (1.9 g/L), and a 0.5 mL trace element solution. The trace element solution contains the following ingredients: $MnSO_4{\cdot}H_2O$ (2.28 g/L), $ZnSO_4{\cdot}7H_2O$ (0.5 g/L), H_3BO_3 (0.5 g/L), $Na_2MoO_4{\cdot}2H_2O$ (0.025 g/L), $CoCl_2{\cdot}6H_2O$ (0.045 g/L), $FeCl_3$ (0.58 g/L), and 0.5 mL of concentrated H_2SO_4. Tris base ($C_4H_{11}NO_3$) was used to buffer the medium. The medium pH was adjusted to 7.2 using 2 M HCl.

3.2. Supporting Media

To verify the kinetic model system, glass beads with diameters of 0.3 cm were selected as the supporting media for denitrifying biomass growth since they do not adsorb acetate and have a precisely known surface area to attach biomass.

3.3. Batch Tests

Two runs from batch experiments for nitrate reduction with acetate degradation performed in 250 mL batch reactors with acclimated denitrifying biomass were placed into an orbital shaker incubator (JSL-530, Lenon Instruments, Taichung, Taiwan) at 120 rpm and 30 °C. The growth of suspended biomass follows log growth, constant growth, and endogenous phases. The growth of suspended biomass under anaerobic conditions is much slower than that under aerobic conditions in batch reactors, thus, the batch reactors were operated for 300 h to observe the endogenous phase for determining the decay coefficients. The initial concentrations of nitrate and acetate were 100 mg NO_3-N/L plus 590 mg acetate/L and 300 mg NO_3-N/L plus 590 mg acetate/L with 18 mg biomass/L in the two batch reactors, respectively. The samples were withdrawn at the onset of the batch tests, and subsequently at suitable time intervals of 6–20 h for measurement of the concentrations of biomass, nitrate, nitrite, and acetate. The two batch kinetic tests were carried out in duplicates.

3.4. Continuous-Flow Bioreactor

Two identical 2.3 L glass reactors equipped with pH and ORP were simultaneously operated to evaluate nitrate reduction with acetate degradation. Experimental data generated in duplicate experiments were used for the validation of the kinetic biofilm model. In order to observe the accumulation of nitrite, the reactors were operated continuously under anaerobic conditions for 54 days. Gu et al. [19] conducted a moving bed biofilm reactor for 60 days to investigate the nitrate removal and nitrite accumulation during the entire process. The nitrate as an electron acceptor and the acetate as an electron donor are two substrates used as carbon and energy sources for the growth of denitrifying biomass [16]. A 160 mL denitrifying biomass with fresh medium was charged into the reactor using a peristaltic pump (Masterflex, Cole Parmer, Vernon Hills, Illinois, USA). The initial concentration of denitrifying biomass in the bioreactor was 0.5 mg biomass/L. The recycle ratio (Q_r/Q) was set at 15 to reach a nearly completely-mixed condition in the fixed-biofilm reactor. The nitrate and acetate at initial concentrations of 150 mg NO_3-N/L and 590 mg acetate/L as well as mineral salt medium were fed into the reactor with an influent flow rate of 640 mL/d. The operating volume of the reactor was 1600 mL, which yields a hydraulic retention time of 2.5 d. The inlet and outlet ports of the water jacket in the outer layer of the reactor were connected to a circulating water bath (Yih Der Inc., Taipei, Taiwan) to maintain the reactor temperature at 28 ± 0.5 °C. One plastic sieve was provided at the top of the reactor to fix glass beads. The dissolved oxygen in the feed tank was removed by purging 99.999% nitrogen gas through a Whatman glass filter (Merck, Damstadt, Germany) to maintain an anaerobic operating condition for the continuous-flow column tests. The pH was controlled at 7.1 ± 0.2 by adding a 50 mM phosphate buffer to the synthetic wastewater. The nitrate and acetate reached a steady-state condition based on the effluent concentration of less than 20% of the initial concentration for at least 20 days. Figure 2 depicts the schematic diagram of fixed-biofilm process for nitrate reduction with acetate degradation.

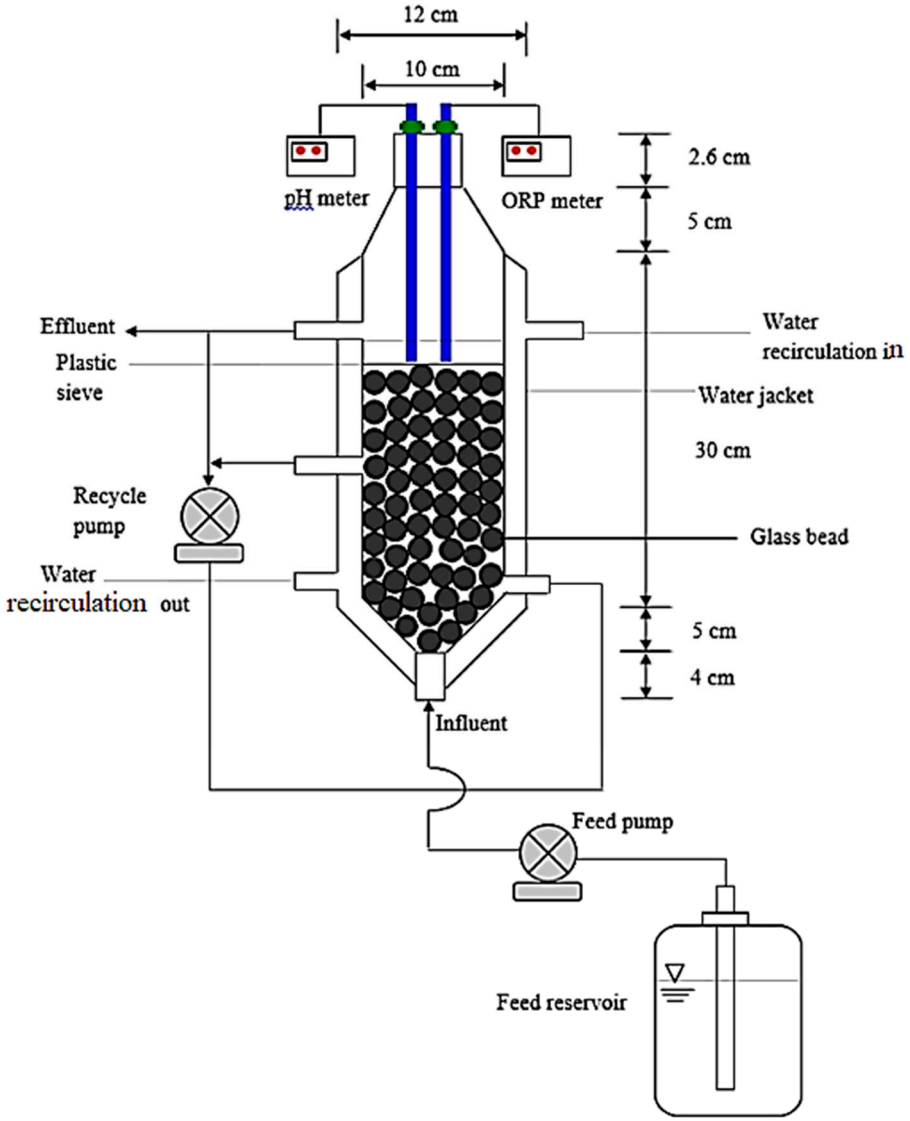

Figure 2. Schematic view of the fixed-biofilm process.

3.5. Analytical Methods

The concentration of microbial growth was determined by measuring the absorbance of samples at 600 nm [9]. The optical density values were converted to biomass concentrations using the linear relationship: X (mg biomass/L) = −1.5379 + 1031.2 × (OD_{600}), R^2 = 0.9933. Liquid samples after filtration with a 0.45 µm membrane filter were analyzed in terms of nitrate, nitrite, and acetate [14]. The concentrations of nitrate-nitrogen (NO_3-N) and nitrite-nitrogen (NO_2-N) in the influent and effluent of batch and fixed-biofilm reactors were measured according to the procedures described in Standard Methods for the Examination of Water and Wastewater [20]. An ultraviolet spectrophotometric screening method at 220 nm and 275 nm was employed to determine the NO_3-N concentration. The linear relationship was represented by the following regression equation: NO_3-N (mg/L) = −0.054221 + 0.38359 × (OD_{220} − 2 × OD_{275}); R^2 = 1.0000. The NO_2-N concentration was analyzed by a colorimetric method at an absorbance value of 543 nm. The NO_2-N concentration adhered to the following regression equation: NO_2-N (mg/L) = −0.0165 + 0.37607 × (OD_{543}); R^2 = 0.9992. The acetate was analyzed using an Agilent model 6850 gas chromatograph equipped with a flame ionization detector. The column was a 6′ × 1/8″ stainless steel column packed with GP 10% SP-1200/1% H_3PO_4 (80/100 mesh). The operating temperatures of the injection port, oven, and detector were maintained at

140, 100, and 140 °C, respectively. Helium, the carrier gas, had a flow rate of 40 mL/min. The acetate concentration was determined by the following equation: acetate (mg/L) = 9.6051 + 0.0079501 × (area); R^2 = 0.9849.

4. Results and Discussion

4.1. Determination of Biokinetic Parameters

Figure 3a,b illustrate the variations of nitrate, nitrite, acetate, and denitrifying biomass concentrations versus operation time in the batch experiments with initial nitrate concentrations of 100 and 300 mg/L at 28 ± 0.5 °C. In both cases, the biomass activity started without any delay, resulting in the utilization of nitrate and acetate and formation of nitrite at similar rates. The removal of nitrite began only when the nitrate concentration dropped to a very low level. In these two cases, nitrate was first reduced to nitrite and then the denitrifying biomass degraded nitrite as an electron acceptor and reduced it to other compounds (i.e., NO, N_2O, and N_2). Acetate utilization and biomass growth occurred in both steps of denitrification. At the initial nitrate concentration of 100 mg/L, although the nitrate was completely reduced, the acetate remained at a constant level of approximately 280 mg/L during the period of 70–300 h at a steady-state condition. However, the nitrate and acetate was fully consumed by the denitrifying biomass at the initial nitrate concentration of 300 mg/L from 70 to 300 h at the steady state. The batch kinetic experiments provided the concentration data of nitrate, nitrite, acetate, and denitrifying biomass, which facilitated a priori estimation of the biokinetic parameters by evaluating the growth rate of the denitrifying biomass and utilization rates of nitrate and acetate. The relevant methods employed for determining the biokinetic parameters from the data of the batch experiments are discussed as follows.

The specific growth rate μ was evaluated from the slope of the growth curve of the denitrifying biomass in the exponential growth phase. The specific growth rate of denitrifying biomass in a batch system, u (1/d) is defined as [21]

$$\mu = \frac{1}{X}\frac{dX}{dt} = \frac{d\ln X}{dt} \tag{15}$$

where is the specific growth rate and X is the biomass concentration (mg/L). By integrating and simplifying Equation (15) it yields the following relation:

$$\mu = \frac{\ln(X_2/X_1)}{t_2 - t_1} \tag{16}$$

where X_1 and X_2 are the cell concentrations at time t_1 and t_2, respectively. The value of the maximum specific growth rate of nitrate reduction (μ_{m,NO_3}) can thus be determined from the slope of a linearized plot of ln$X$ versus time in the log phase [20]. The values of μ_{m,NO_3} were equal to 0.329 and 0.539 1/d at the two initial nitrate concentrations of 100 and 300 mg NO_3-N/L, respectively (Figure 4).

The biomass yield Y (mg biomass/mg substrate) was assumed approximately constant over the range of substrate concentrations encountered in the growth phase. The biomass yield on nitrate reduction and acetate degradation can be determined using the following equation [22]:

$$Y = \frac{(X_M - X_0)}{(S_M - S_0)} \tag{17}$$

where X_M and X_0 are the maximum and initial dry biomass concentrations, respectively, and S_M and S_0 are the substrate concentrations at the maximum biomass concentration and initial substrate concentration, respectively. The slope of a linearized plot of the increase in denitrifying biomass (ΔX) versus the decrease in nitrate concentration (ΔS) represented the denitrifying biomass yield by nitrate, as presented in Figure 5. The nitrate biomass yields (Y_{NO_3}) were 0.936 and 0.985 mg biomass/mg nitrate, respectively. The slope of a linearized plot obtained from the denitrifying biomass increase versus acetate decrease represented acetate biomass yields on nitrate reduction (Y_{Ace-NO_3}), which were 0.0168

and 0.0209 mg biomass/mg acetate at the initial nitrate concentrations of 100 and 300 mg NO_3-N/L, respectively (Figure 6).

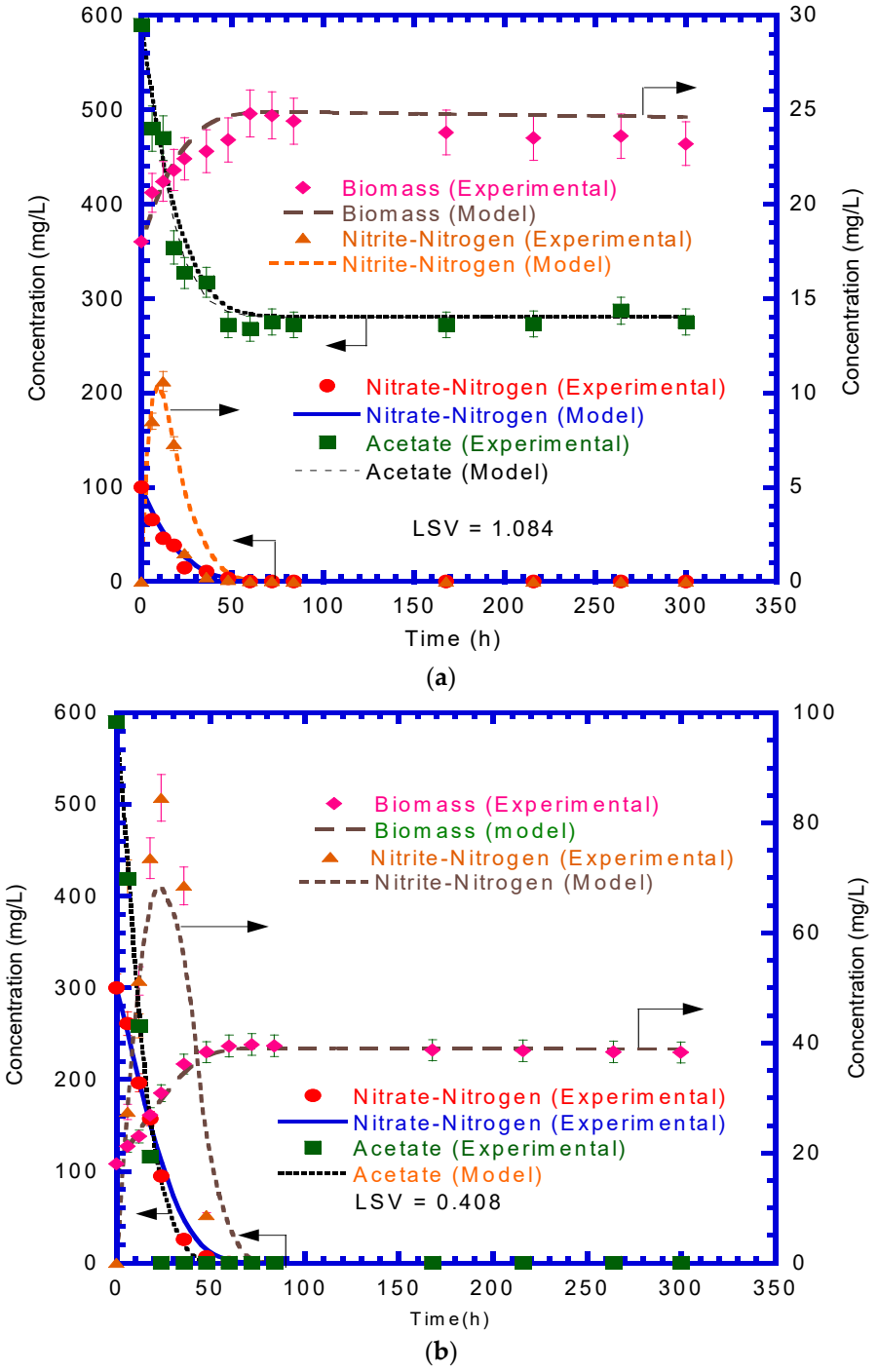

Figure 3. Batch denitrification at initial nitrate-nitrogen concentration of (**a**) 100 mg/L and (**b**) 300 mg/L. Symbols are the average value of the data obtained in duplicate experiments and error bars are the associated standard deviations. Solid and dash lines represent the model prediction.

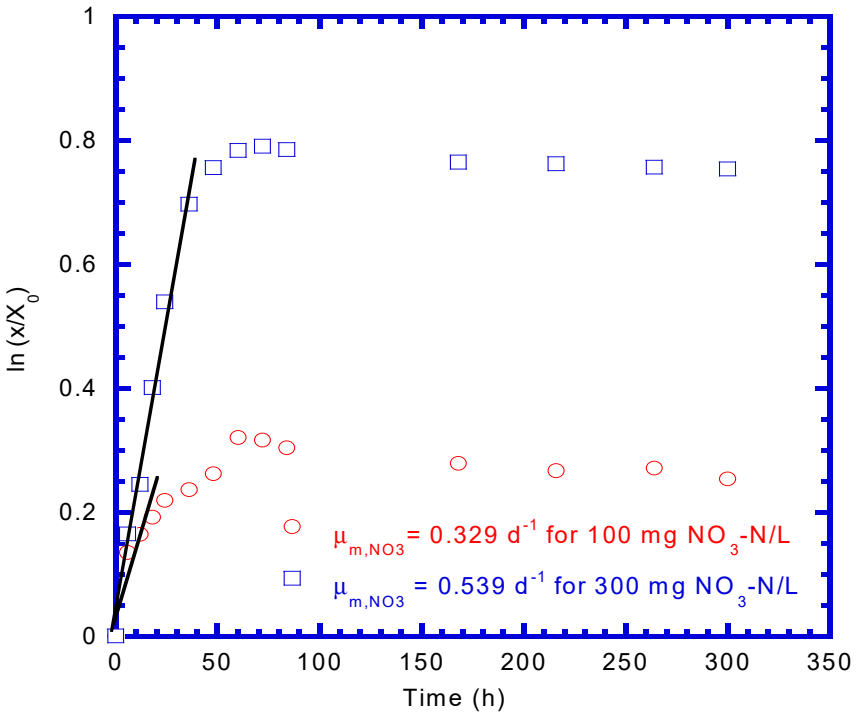

Figure 4. Batch kinetic test to determine maximum specific growth rate of denitrifying biomass at different initial nitrate concentrations of 100 and 300 mg NO_3-N/L.

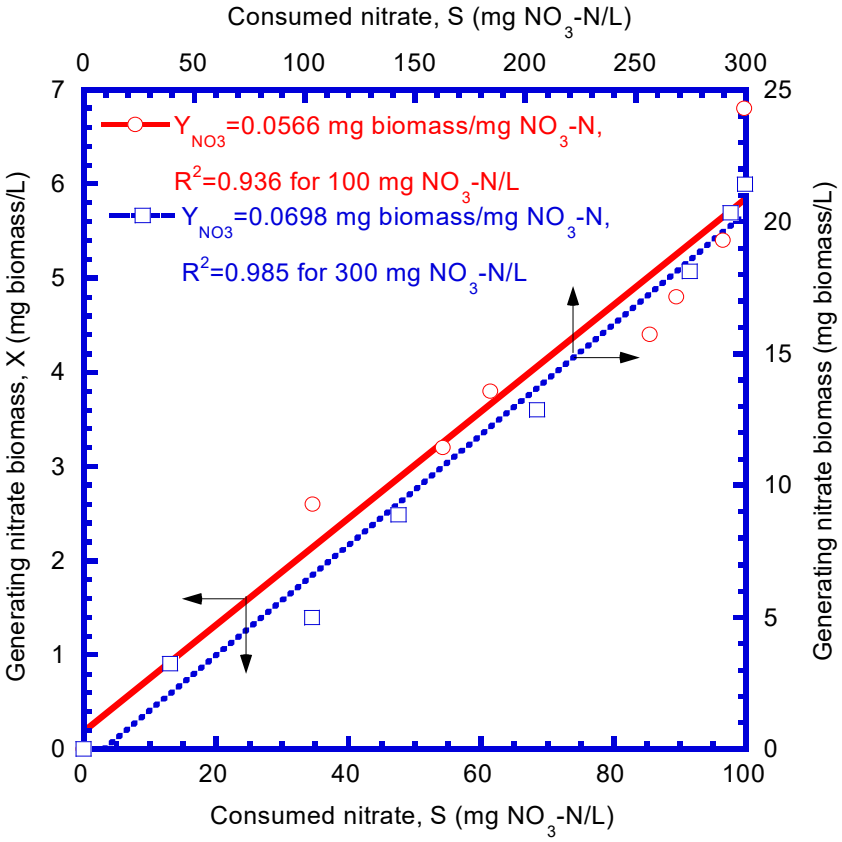

Figure 5. Batch kinetic test to determine nitrate biomass yield at different initial nitrate concentrations of 100 mg and 300 mg NO_3-N/L.

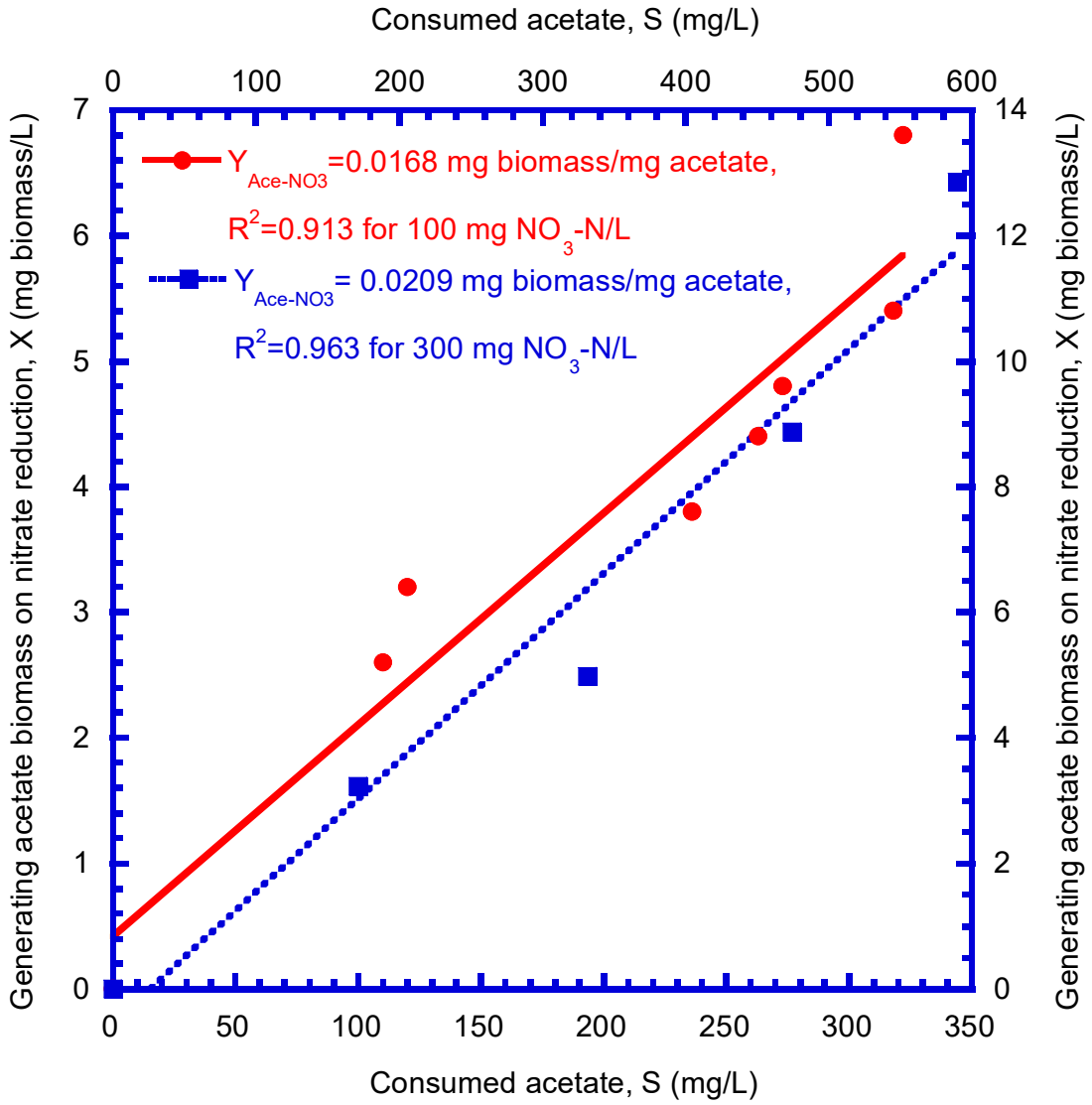

Figure 6. Batch kinetic test to determine acetate biomass yield at different initial nitrate concentrations of 100 and 300 mg NO_3-N/L.

The experimental data of denitrifying biomass concentrations in the endogenous phase were applied to evaluate the decay coefficient (b) of the denitrifying biomass. In the endogenous phase, the denitrifying biomass concentration decreased with time and the decay coefficient (b) of the denitrifying biomass can be expressed as determined previously from the slope of a linearized plot of lnX versus time. The decay coefficient (b) can be represented by the following equation [23]:

$$b = -\frac{\ln(X_2/X_1)}{t_2 - t_1} \tag{18}$$

where X_1 and X_2 are the biomass concentrations at time t_1 and t_2, respectively. The decay coefficient evaluated from the slope of a linearized plot of lnX versus time in the endogenous phase is depicted in Figure 7. The values of the decay coefficient of the nitrate biomass (b_{NO_3}) were 6.24×10^{-3} and 3.81×10^{-3} 1/d, respectively, at the initial nitrate concentrations of 100 and 300 mg NO_3-N/L (Figure 7).

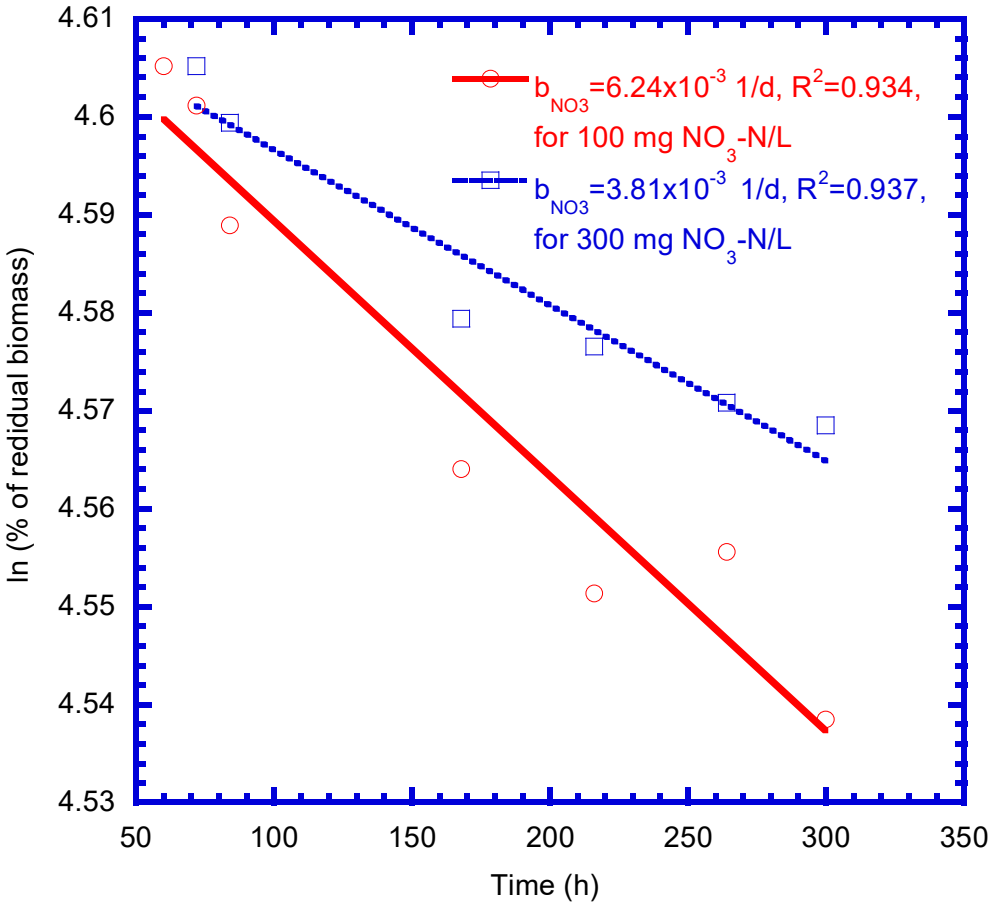

Figure 7. Batch kinetic tests to determine decay coefficient of denitrifying biomass at different initial nitrate concentrations of 100 and 300 mg NO_3-N/L.

The nitrate utilization rate described by Monod kinetics was used to determine the value of the half-saturation constant (K_s) for nitrate. The nitrate utilization rate by denitrifying biomass at time zero can be represented by the following equation:

$$\left.\frac{dS}{dt}\right|_{t=0} = \frac{-\mu_m S_0 X_0}{Y(K_S + S_0)} \tag{19}$$

After arrangement, the K_S value can be determined by the following equation:

$$K_S = -S_0\left[1 + \frac{\mu_m}{Y} X_0 \left(\frac{dS}{dt}\right)_0^{-1}\right] \tag{20}$$

The slope of the nitrate utilization curve at time zero was taken to compute the values of the half-saturation constant for nitrate (K_{S,NO_s}), which were 266.2 and 186.5 mg NO_3-N/L at the initial nitrate concentrations of 100 and 300 mg NO_3-N/L, respectively.

Furthermore, the biokinetic parameters including the maximum specific growth rate of nitrite reduction (μ_{m,NO_2}), nitrite biomass yield (Y_{NO_2}), acetate biomass yield on nitrite reduction (Y_{Ace-NO_2}), Monod half-saturation constant of nitrite (K_{S,NO_2}), and decay coefficient of nitrite biomass (b_{NO_2}) were evaluated by the Monod kinetic model system expressed as Equations (2)–(5) in Section 2.1. The simulated results of Monod kinetic equations were fitted to the experimental data using the LSV technique presented in Equation (6). The values of μ_{m,NO_2}, Y_{NO_2}, Y_{Ace-NO_2}, K_{S,NO_2}, and b_{NO_2} obtained from the fitted model are listed in Table 1.

Table 1. Biokinetic parameters based on the batch experimental data and model fitted.

Symbol	Parameter Description (Unit)	Nitrate Concentration (mg/L)		Average
		100	300	
μ_{m,NO_3}	Maximum specific growth rate of nitrate reduction (1/d)	0.329	0.539	0.434
μ_{m,NO_2}	Maximum specific growth rate of nitrite reduction (1/d)	0.120	0.122	0.121
Y_{NO_3}	Nitrate biomass yield (mg biomass/mg NO_3–N)	0.0566	0.0698	0.0632
Y_{NO_2}	Nitrite biomass yield (mg biomass/mg NO_2–N)	0.0217	0.0225	0.0221
Y_{Ace-NO_3}	Acetate biomass yield on nitrate reduction (mg biomass/mg acetate)	0.0168	0.0209	0.0189
Y_{Ace-NO_2}	Acetate biomass yield on nitrite reduction (mg biomass/mg acetate)	0.0847	0.0794	0.0821
K_{S,NO_3}	Monod half saturation constant of nitrate (mg NO_3–N/L)	266.2	186.5	226.35
K_{S,NO_2}	Monod half saturation constant of nitrite (mg NO_2–N/L)	4.14	4.32	4.23
b_{NO_3}	Decay coefficient of nitrate biomass (1/d)	6.24×10^{-3}	3.81×10^{-3}	5.03×10^{-3}
b_{NO_2}	Decay coefficient of nitrite biomass (1/d)	6.4×10^{-4}	2.6×10^{-4}	4.5×10^{-4}

4.2. Determination of Mass Transfer Coefficients

The diffusion coefficients in the biofilm are generally less than those in the bulk liquid phase due to the diffusional resistance to the transport of the substrates, which is posed by bacteria and their extracellular materials. Thus, the diffusion coefficient in the biofilm was obtained by multiplying the diffusion coefficient in the bulk liquid phase (D_w) by a factor of 0.8 to correct the diffusional resistance in the biofilm [24]. The empirical correlation of Wilke and Chang [25] was used to compute the diffusion coefficients of nitrate, nitrite, and acetate in bulk liquid (D_w). The empirical formula can be described as follows:

$$D_w = 7.4 \times 10^{-8} \frac{(\phi_b M_b)^{0.5} T}{\mu_b {V_b}^{0.6}} \tag{21}$$

where φ_b is the association constant, M_b is the molecular weight of water, T is the absolute temperature (K), μ_b is the absolute viscosity (cP) of the solution for water, and V_b is the molar volume of the solute as liquid at its normal boiling point and is estimated from the atomic volume of their atoms [26]. For nitrate, nitrite, and acetate, the V_b values are 37.8, 30.4, and 55.5 cm^3/mol. Therefore, the diffusion coefficients of nitrate, nitrite, and acetate in the biofilm were 1.326, 1.509, and 1.051 cm^2/day, respectively [24].

The empirical expression used to evaluate the liquid-film transfer coefficient (k_f) for the packed-bed reactor can be calculated by the following equation [27]:

$$k_f = 1.17 v_s (R_e)^{-0.42} (S_c)^{-0.67} \tag{22}$$

where v_s is the superficial flow velocity (cm/d) through the reactor, $R_e = \frac{d_p v_s}{\upsilon}$ is the Reynolds number (dimensionless), $S_c = \frac{\upsilon}{D_w}$ is the Schmidt number (dimensionless), d_p is the diameter (cm) of the glass bead, and υ is the kinematic viscosity of water (cm^2/d). The computed values of the liquid-film transfer coefficients for nitrate, nitrite, and acetate were 349.41, 381.07, and 299.14 cm/d, respectively.

The specific shear-loss coefficient (b_s) of the biofilm on the glass bead can be evaluated via the following empirical formula [28]:

$$b_s = 2.29 \times 10^{-6} \left[\frac{\upsilon v_s (1-\varepsilon)^3}{{d_p}^2 \varepsilon^3 a} \right]^{0.58} \tag{23}$$

where υ is the kinematic viscosity of water (cm^2/d), and a is the specific surface area of the column bed (1/cm). The computed value of b_s was equal to 2.71×10^{-2} 1/d.

4.3. Nitrate Reduction with Acetate Degradation

The model was validated by evaluating the nitrate reduction with acetate degradation by conducting a column test fed with a nitrate concentration of 150 mg/L and the acetate concentration of 590 mg/L. The kinetic parameters determined from the various batch kinetic experiments and the mass transfer coefficients evaluated by the empirical formula calculation for the biofilm model prediction are listed in Table 2.

Table 2. Biokinetic and reactor parameters as well as mass transfer coefficients used in the biofilm model prediction.

Parameter	Value
Measured	
Acetate biomass yield on nitrate reduction, Y_{Ace-NO_3}(mg biomass/mg acetate)	0.0189
Acetate concentration in the feed, $S_{b0,Ace}$(mg/L)	590
Concentration of suspended nitrifying biomass in the reactor, X_{b0}(mg biomass/L)	0.5
Decay coefficient of nitrate biomass, b_{NO_3}(1/d)	5.03×10^{-3}
Density of nitrifying biofilm, X_f(mg biomass/L)	10.64
Effective working volume, V(mL)	1.6×10^3
Influent flow rate, Q(mL/d)	640
Maximum specific growth rate of nitrate reduction, μ_{m,NO_3}(1/d)	0.434
Nitrate biomass yield, Y_{NO_3}(mg biomass/mg NO_3-N)	0.0632
Nitrate-nitrogen concentration in the feed, S_{b0,NO_3}(mg/L)	150
Reactor porosity (dimensionless)	0.43
Fitted	
Acetate biomass yield on nitrite reduction, Y_{Ace-NO_2}(mg biomass/mg acetate)	0.0821
Decay coefficient of nitrite biomass, b_{NO_2}(1/d)	4.5×10^{-4}
Maximum specific growth rate of nitrite reduction, μ_{m,NO_2}(1/d)	0.121
Monod half-saturation constant of nitrite, K_{S,NO_2}(mg NO_2-N/L)	4.23
Nitrite biomass yield, Y_{NO_2}(mg biomass/mg NO_2-N)	0.0221
Calculated	
Diffusion coefficient of acetate, $D_{f,Ace}$(cm^2/d)	1.051
Diffusion coefficient of nitrate, D_{f,NO_3}(cm^2/d)	1.326
Diffusion coefficient of nitrite, D_{f,NO_2}(cm^2/d)	1.509
Liquid film transfer coefficient of acetate, $k_{f,Ace}$(cm/d)	299.14
Liquid film transfer coefficient of nitrate, k_{f,NO_3}(cm/d)	349.41
Liquid film transfer coefficient of nitrite, k_{f,NO_2}(cm/d)	381.07
Monod half-saturation constant of nitrate, K_{S,NO_3}(mg NO_3-N/L)	226.35
Specific shear-loss coefficient of denitrifying biomass, b_s(1/d)	2.71×10^{-2}
Total surface area of glass beads, A(cm^2)	1.829×10^4
Assumed	
Initial denitrifying biofilm thickness, L_{f0}(μm)	1.5

Figure 8a,b indicate that the effluent concentrations of nitrate and acetate varied over time. The variation curves of the nitrate and acetate concentrations can be divided into three segments. The nitrate and acetate concentrations first increased abruptly to approximately 119.4 mg NO_3-N/L (0.796 S_{b0,NO_3}) and 439.6 mg acetate/L (0.745 $S_{b0,Ace}$) at 4 d, respectively. No significant nitrate reduction with acetate degradation was observed at this period. The substrate-concentration curve represented as a typical dilute-in curve was a property of the completely-mixed flow reactor while the reactor was filled with mineral nutrient media only at time zero.

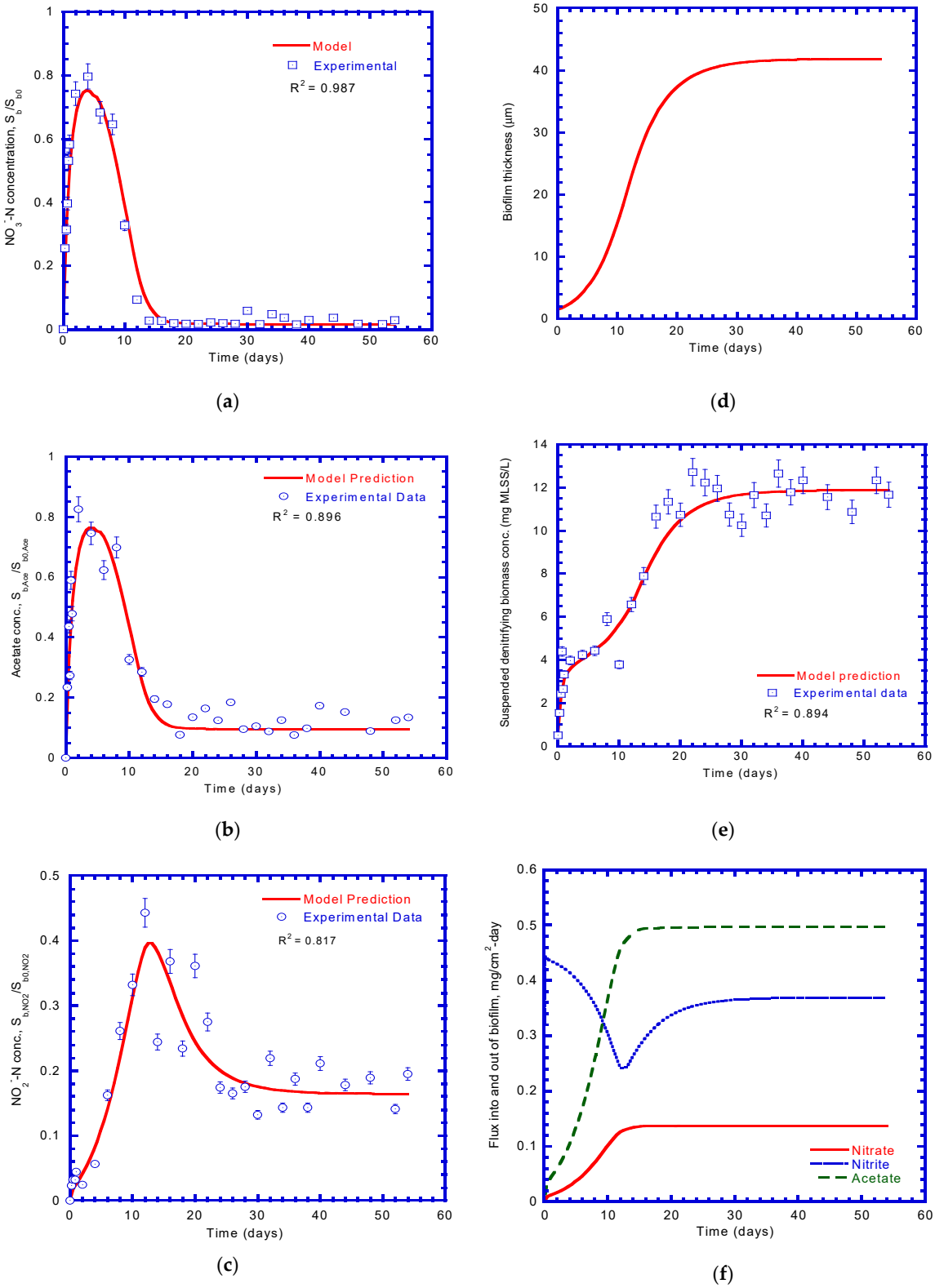

Figure 8. Experimental data and model predictions in the biofilm system: (**a**) nitrate effluent, (**b**) acetate effluent, (**c**) nitrite effluent, (**d**) biofilm growth, (**e**) suspended biomass growth, and (**f**) flux into and out of the biofilm.

The second segment of the nitrate and acetate curves ran from 4 to 18 d, when the concentration curves started to deviate from the dilute-in curve of the reactor. The effluent concentration curves of

nitrate and acetate leveled off and then gradually decreased. Apparently, the denitrifying biofilm was actively utilizing nitrate and acetate for denitrification during this stage. The denitrifying biofilm was also vigorously growing during this stage.

The third segments of the nitrate and acetate curves ran from 18 to 54 d. In this period, the system reached a steady-state condition and the effluent concentrations of nitrate and acetate were approximately 2.39 mg NO_3-N/L (0.0159 S_{b0,NO_3}) and 55.8 mg acetate/L (0.0946 $S_{b0,Ace}$), respectively. The removal efficiency of nitrate was 98.4% accompanied with 90.5% acetate consumption in a steady-state condition.

The variation of the formation and biodegradation of nitrite with time is illustrated in Figure 8c. The first segment of the curve ran from 0 to 12 d. In this period, the nitrite production rate by biomass was higher than its utilization rate by biomass. The peak height of nitrite concentration was 66.45 mg NO_2-N/L (0.443 S_{b0,NO_3}). At the second segment, in a range of 12–30 d, the nitrite concentration gradually decreased since the nitrite production rate was lower than the nitrite utilization rate. At the third segment, in a range of 30–54 d, the nitrite production rate was almost the same as the nitrite utilization rate; therefore, the system reached a steady-state condition. At the steady-state condition, the nitrite effluent concentration was about 26.3 mg NO_2-N/L (0.175 S_{b0,NO_3}).

Several studies have shown that biofilm processes have a high capacity for removing nitrate. Lazarova et al. [29] conducted two denitrifying fluidized bed reactors with different enrichment cultures as inoculum and fed continuously with 30 ± 5 mg NO_3-N/L to investigate the nitrate removal efficiency at the steady state. The experimental results indicated that a high nitrate removal efficiency of 97–100% was achieved at a steady-state condition. However, they found that approximately 30% of the initial nitrate fed was reduced to nitrite and accumulated in the fluidized bed reactor. The nitrate removal efficiency was close to that obtained from this study; however, a higher percentage of nitrite accumulation was observed in their study.

4.4. Growth of Denitrifying Biomass

Figure 8d exhibits the variation of the growth curve of the denitrifying biofilm with time by the model prediction from the non-steady-state to the steady-state condition. The time needed for the biofilm to initiate growth was nearly 2 d. The biofilm grew vigorously to reduce nitrate from 2 to 25 d. At the steady-state condition, the maximal biofilm thickness reached up to 41.8 μm by the model prediction.

Figure 8e illustrates the variation of the growth curve of the suspended biomass with time. The effluent concentration of suspended biomass is one index of the biomass generation in the continuous-flow reactor. The concentration of suspended biomass in the effluent, which was predicted by the model, was similar to the experimental values obtained from the continuous-flow column test. The agreement between experimental and model results was satisfactory. The variation of the growth curves of the suspended and attached biomass with time was similar, indicating that the biofilm and suspended biomass simultaneously utilized the substrates in the reactor. The growth rate of suspended biomass rapidly increased during an unsteady-state period of 2–25 d, in which the suspended biomass actively degraded the substrates for growth. The highest effluent concentration of suspended denitrifying biomass occurring in a steady-state condition was approximately 11.9 mg biomass/L.

Figure 8f plots the fluxes by model prediction for nitrate, nitrite, and acetate through the interface at the liquid film/biofilm with operating time. The plot shows that the nitrate and acetate fluxes increased with time and reached the steady state. At the onset of the column test, the growth of biofilm was insignificant and the diffusional resistance was minimal; thus, the substrate concentration gradient between bulk liquid and biofilm was negligible. As the biofilm grew thicker, it utilized nitrate and acetate; thus, both substrate concentrations at the liquid film/biofilm interface became lower. At this stage, the high concentration gradient caused the flux to have a marked increase. The biofilm thickness remained constant due to the same growth rate and decay rate at the steady state. This resulted in

a constant concentration gradient; thus, the fluxes of nitrate and acetate maintained the same values, i.e., 0.137 and 0.497 mg/cm^2-d, respectively.

It is noted that the nitrite flux diffused out of the biofilm (Figure 8f). In the first step of denitrification, as the biofilm grew thicker, more nitrite was produced and accumulated in the biofilm. At this stage, the nitrite concentration gradient steadily decreased to cause the nitrite flux to diffuse out of the biofilm. In the second step of denitrification, the nitrite concentration accumulating in the biofilm was steadily degraded by the biofilm; thus, the nitrite concentration gradient gradually increased back to a steady-state level. The nitrite flux at a steady-state condition was 0.369 mg/cm^2-d.

4.5. Concentration Profiles of Nitrate and Acetate

Figure 9 depicts the nitrate and acetate concentration profiles in the liquid film and biofilm on day 50. The nitrate and acetate diffused through the liquid film into the biofilm to exhibit concentration profiles that were formed by a diffusional resistance. On day 50, the bioreactor performance reached a steady state. The concentrations of nitrate and acetate at the liquid film were 2.39 mg NO_3-N/L (0.0159 S_{b0,NO_3}) and 55.8 mg acetate/L (0.0946 $S_{b0,Ace}$), respectively. The concentration profiles of nitrate and acetate rapidly decreased to approximately zero near the solid surface of the glass bead. The concentrations of nitrate and acetate at the solid surface were 1.77 mg NO_3-N/L (0.0118 S_{b0,NO_3}) and 53.87 mg acetate/L (0.0913 $S_{b0,Ace}$), respectively. On day 50, the biofilm was identified as a "deep biofilm" at a steady-state condition [30].

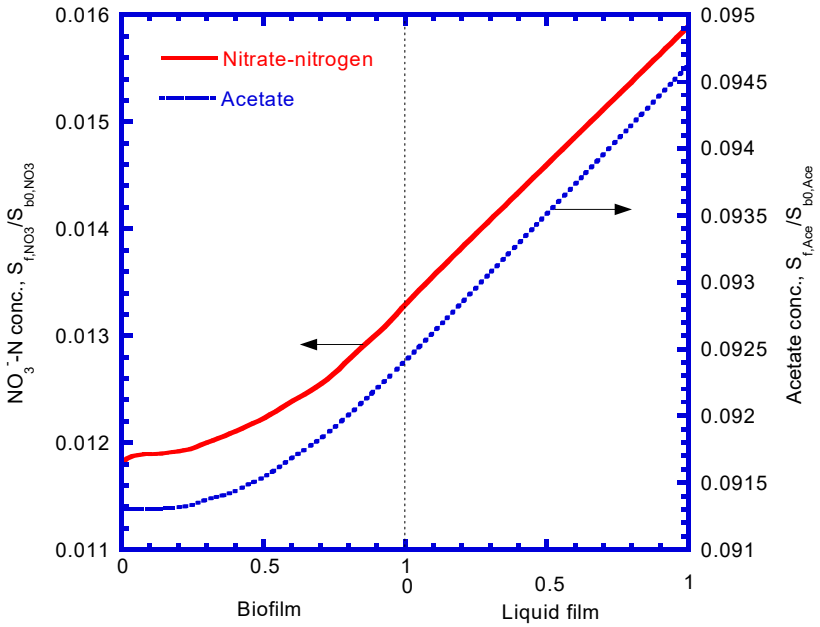

Figure 9. Concentration profiles of nitrate and acetate in the liquid film and biofilm.

5. Conclusions

The kinetic model system was derived to describe the nitrate reduction, nitrite production and utilization, and acetate biodegradation by the denitrifying biomass in the biofilm reactor. The completely-mixed, continuous-flow biofilm reactor was used to validate the model. The experimental data and model predictions of the effluent concentrations of nitrate, nitrite, and acetate agreed satisfactorily with each other. The biofilm reactor was capable of achieving a high removal of nitrate at feed concentrations of 150 mg/L nitrate and 590 mg/L acetate. The removal efficiency of nitrate was 98.4% accompanied with 90.5% acetate consumption in a steady-state condition. The combination of the orthogonal collocation method and Gear's method was an efficient numerical technique to solve the continuous-flow fixed-biofilm model from a non-steady-state to steady-state condition.

The kinetic model was also a powerful tool for designing the biological process and improving the process control. The modeling and experimental approaches used in this study could be applied in the design of a pilot-scale, or full-scale, fixed-biofilm reactor for nitrate removal in water and wastewater treatment plants.

Author Contributions: Y.-H.L. conceived and designed the experiments as well as developed the kinetic models and solved the model and analyzed the experimental data; Y.-J.G. performed the experiments and collected the data. All authors have read and agreed to the published version of the manuscript.

Funding: This research was supported in part by a grant from the Ministry of Science and Technology of Taiwan under Contract No. MOST 108-2221-E-166-002.

Conflicts of Interest: The authors declare no conflict of interest.

References

1. Karanasios, K.A.; Vasiliadou, I.A.; Pavlou, S.; Vayenas, D.V. Hydrogenotrophic denitrification of potable water: A review. *J. Hazard. Mater.* **2010**, *180*, 20–37. [CrossRef] [PubMed]
2. Liu, X.; Huang, M.; Bao, S.; Tang, W.; Fang, T. Nitrate removal from low carbon-to-nitrogen ratio wastewater by combining iron-based chemical reduction and autotrophic denitrification. *Bioresour. Technol.* **2020**, *301*, 1–8. [CrossRef] [PubMed]
3. Fernández-Nava, Y.; Marañón, E.; Soons, J.; Castrillón, L. Denitrification of wastewater containing high nitrate and calcium concentrations. *Bioresour. Technol.* **2008**, *99*, 7976–7981. [CrossRef] [PubMed]
4. Saliling, W.J.B.; Westerman, P.W.; Losordo, T.M. Wood chips and wheat straw as alternative biofilter media for denitrification reactors treating aquaculture and other wastewaters with high nitrate concentrations. *Aquacult. Eng.* **2007**, *37*, 222–233. [CrossRef]
5. Honda, H.; Watanabe, Y.; Kikuchi, K.; Iwata, N.; Takeda, S.; Uemoto, H.; Furuta, T.; Kiyono, M. High density rearing of Japanese flounder, *Paralichthys olivaceus* with a closed seawater recirculation system equipped with a denitrification unit. *Aquacult. Sci.* **2010**, *41*, 19–26.
6. Ayyasamy, P.M.; Rajakumar, S.; Sathishkumar, M.; Swaminathan, K.; Shanthi, K.; Lakshmanaperumalsamy, P.; Lee, S. Nitrate removal from synthetic medium and groundwater with aquatic macrophytes. *Desalination* **2009**, *242*, 286–296. [CrossRef]
7. Jang, C.S.; Chen, S.K. Integrating indicator-based geostatistical estimation and aquifer vulnerability of nitrate-N for establishing groundwater protection zones. *J. Hydrol.* **2015**, *523*, 441–451. [CrossRef]
8. Wang, Q.; Feng, C.; Zhao, Y.; Hao, C. Denitrification of nitrate contaminated groundwater with a fiber-based biofilm reactor. *Bioresour. Technol.* **2009**, *100*, 2223–2227. [CrossRef]
9. Rezvani, F.; Sarrafzadeh, M.H.; Ebrahimi, S.; Oh, H.M. Nitrate removal from drinking water with a forcus on biological methods: A review. *Environ. Sci. Pollut. Res.* **2019**, *26*, 1124–1141. [CrossRef] [PubMed]
10. Ersever, I.; Ravindran, V.; Pirbazari, M. Biological denitrification of reverse osmosis brine concentrates: I. Batch reactor and chemostat studies. *J. Environ. Eng. Sci.* **2007**, *6*, 503–518. [CrossRef]
11. Tang, K.; Baskaran, V.; Nemati, M. Bacteria of the sulphur cycle: An overview of microbiology, biokinetics and their role in petroleum and mining industries. *Biochem. Eng. J.* **2009**, *44*, 73–94. [CrossRef]
12. Biradar, P.M.; Roy, S.B.; D'Souza, S.F.; Pandit, A.B. Excess cell mass as an internal carbon source for biological denitrification. *Bioresour. Technol.* **2010**, *101*, 1787–1791. [CrossRef] [PubMed]
13. Nadeem, S.; Dörsch, P.; Bakken, R. Autoxidation and acetylene-accelerated oxidation of NO in a 2-phase system: Implications for the expression of denitrification in ex situ experiments. *Soil Biology Biochem.* **2013**, *57*, 606–614. [CrossRef]
14. Vasiliadou, I.A.; Pavlou, S.; Vayenas, D.V. A kinetic study of hydrogenotrophic denitrification. *Process. Biochem.* **2006**, *41*, 1401–1408. [CrossRef]
15. Soto, O.; Aspé, E.; Roeckel, M. Kinetics of cross-inhibited denitrification of a high load wastewater. *Enzym. Microb. Technol.* **2007**, *40*, 1627–1634. [CrossRef]
16. An, S.K.; Stone, H.; Nemati, M. Biological removal of nitrite by an oil reservoir culture capable of autotrophic and heterotrophic activities: Kinetic evaluation and modeling of heterotrophic process. *J. Hazard. Mater.* **2011**, *190*, 686–693. [CrossRef]

17. Gear, C.W. The automatic integration of ordinary differential equations. *Commun. ACM* **1971**, *14*, 176–179. [CrossRef]
18. Skoneczny, S.; Cioch-Skoneczny, M. Mathematical modeling and approximate solutions for microbiological processes in bioifilm through homotopy-based methods. *Chem. Eng. Res. Des.* **2018**, *139*, 309–320. [CrossRef]
19. Gu, W.; Wang, L.; Liu, Y.; Liang, P.; Zhang, X.; Li, Y.; Huang, X. Anammox bacteria enrichment and denitrification in moving bed biofilm reactors packed with different buoyant carriers: Performances and mechanisms. *Sci. Total Environ.* **2020**, *719*, 1–11. [CrossRef]
20. APHA. *Standard Method for the Examination of Water and Wastewater*, 21st ed.; American Public Health Association: Washington, DC, USA, 2005.
21. Koutinas, M.; Kiparissides, A.; Lam, M.C.; Silva-Rocha, R.; Godinho, M.; de Lorenzo, V.; dos Santos, V.A.P.M.; Pistikopoulos, E.N.; Mantalaris, A. Improving the prediction of *Pseudomonas putida* mt-2 growth kinetics with the use of a gene expression regulation model of the TOL plasmid. *Biochem. Eng. J.* **2011**, *55*, 108–118. [CrossRef]
22. Abuhamed, T.; Bayraktar, E.; Mehmetoğlu, T.; Mehmetoğlu, Ü. Kinetics model for growth of *Pseudomonas putida* F1 during benzene, toluene and phenol biodegradation. *Process. Biochem.* **2004**, *39*, 983–988. [CrossRef]
23. Sivarajan, P.; Arutchelvan, V.; Nagarajan, S. Biodegradation kinetics of 2-chlorophenol with starch water as co-substrate using anaerobic batch reactor. *Inter. J. Eng. Res. Technol.* **2016**, *5*, 141–145. [CrossRef]
24. Williamson, K.; McCarty, P.L. Verification studies of the biofilm model for bacterial substrate utilization. *J. Water Pollut. Control. Fed.* **1976**, *48*, 281–296.
25. Wilke, C.E.; Chang, P. Correlation of diffusion coefficients in dilute solutions. *Aiche J.* **1955**, *1*, 264–270. [CrossRef]
26. Perry, R.H.; Chilton, C.H. *Chemical Engineers Handbook*, 5th ed.; McGraw-Hill: New York, NY, USA, 1973; pp. 3–229.
27. Cussler, E.L. *Diffusion, Mass Transfer in Fluid Systems*, 2nd ed.; Cambridge University Press: New York, NY, USA, 1997.
28. Speitel, G.E., Jr.; DiGiano, F.A. Biofilm shearing under dynamic conditions. *J. Environ. Eng. ASCE* **1987**, *113*, 464–475. [CrossRef]
29. Lazarova, V.; Capdeville, B.; Nikolov, L. Influence of seeding conditions on nitrite accumulation in a denitrifying bed reactor. *Water Res.* **1994**, *28*, 1189–1197. [CrossRef]
30. Jiang, F.; Leung, D.H.W.; Li, S.; Chen, G.H.; Okabe, S.; van Loosdrecht, M.C.M. A biofilm model for prediction of pollutant transformation in sewers. *Water Res.* **2009**, *43*, 3187–3198. [CrossRef]